A Framework for Fault Diagnosis in Managed Pressure Drilling Applied to Flow-Loop Data

Anders Willersrud * **Lars Imsland** * **Alexey Pavlov** ** **Glenn-Ole Kaasa** **

* *Department of Engineering Cybernetics, Norwegian University of Science and Technology, N-7491 Trondheim, Norway (email: [anders.willersrud, lars.imsland]@itk.ntnu.no).*
** *Department of Intelligent Drilling, Statoil Research Centre, N-3905 Porsgrunn, Norway (email: [alepav, gkaa]@statoil.com).*

Abstract: Data from a medium-scale horizontal flow loop test facility is used to test fault diagnosis in managed pressure drilling. The faults are downhole incidents such as formation influx, fluid loss, drillstring washout, pack-off, and plugging of the drill bit, which are important to detect and handle in order to avoid downtime and possibly dangerous situations. In this paper a fault diagnosis scheme based on an adaptive observer and the generalized likelihood ratio test is applied on the experimental data. The different types of faults are detected and their location are isolated using friction parameter estimates. Results indicate that the method can in most cases identify the type of fault, whereas the location is sometimes more uncertain.

Keywords: Fault diagnosis, managed pressure drilling, flow loop, nonlinear adaptive observer

1. INTRODUCTION

Drilling for oil and gas is always associated with risk. As reservoirs become depleted or more difficult to reach, operations become more complex, and safety margins smaller. It will then be increasingly important to improve monitoring and control of the downhole drilling process to avoid incidents and reduce downtime. In drilling the pressure in the well must be carefully monitored and controlled to be above the formation pore pressure and below its fracture pressure. If the pressure is lower than the pore pressure, formation fluids can start flowing into the well. If the pressure becomes too high, the formation can start to fracture leading to losses of drilling fluid ("mud") to the formation, damaging the reservoir. Managed pressure drilling (MPD) is a method which seals off the annulus around the drillstring and routes the return flow of the drilling fluid through a controlled choke, making it possible to more carefully control the downhole pressure. See Fig. 1 for a schematic overview. With this technology it is possible to drill wells with narrow pressure margins. In this case, detection and handling abnormal situation becomes very important.

A situation which is critical to detect is an influx of reservoir fluids, also known as a kick. An influx can happen if some parts of the wellbore become underbalanced, i.e., with well pressure below formation pore pressure. If gas enters the annulus, the hydrostatic pressure will decrease due to lower mixed density. This can in turn increase the influx, making the situation worse. If continued uncontrolled, the situation can develop into a blowout, which is an uncontrolled flow of reservoir fluids into the well and must be prevented at all costs. One of the causes

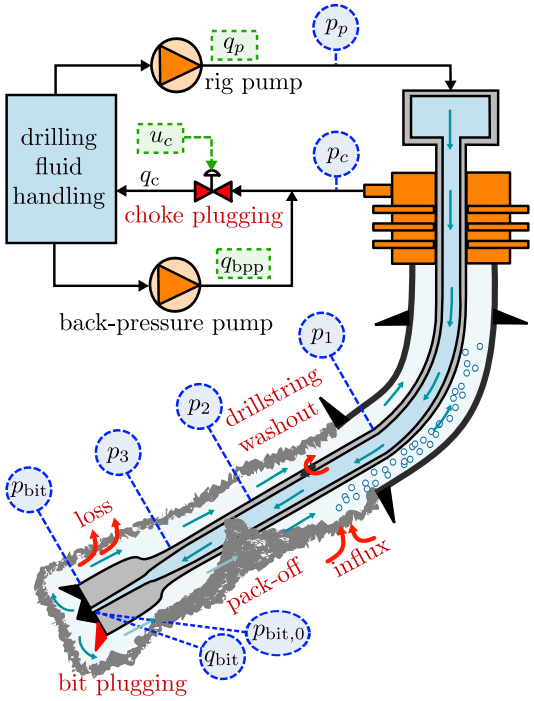

Fig. 1. Managed pressure drilling with possible faults. Measurements are labeled in blue, actuators in green.

for the well to become underbalanced is lost circulation of drilling fluid. If enough fluid is lost, the back-pressure is lost which will decrease the hydrostatic head in the annulus. Poor transport or accumulation of cuttings can result in formation of a pack-off, which in turn changes the annular friction and can also result in a stuck pipe. Moreover, lost circulation of drilling fluid is important

from a cost perspective since the drilling fluid can contain expensive chemicals. In addition to being a safety risk, the mentioned incidents will increase the nonproductive time during drilling, which on average is 20-25 % of the drilling time and thus a major cost (Godhavn, 2010).

In this paper, data from a medium-scale flow loop is used to study contingency and fault diagnosis in managed pressure drilling. The test setup is made to mimic a real drilling process as closely as possible, and manages to reproduce many of the possible faults in a realistic manner. The faults we study are illustrated in Fig. 1, which all cause changes in pressure. Some faults are also related to changes of mass flow through the system, such as influx and lost circulation. In addition to topside pressure measurements, distributed pressure sensors is used along the drill pipe. This is a rather new communication technology called wired drill pipe, which increases the number of measurement points as well as data bandwidth (Nygaard et al., 2008). These measurements are used in an adaptive observer to estimate friction parameters throughout the system. Applying a detection algorithm on the estimated friction parameters, it is possible to detect and isolate the different faults causing changes to friction and flow. The position is isolated to be in between two pressure sensors. This is done without using a flow meter downstream the choke.

Detection of influx and loss is studied in Hauge et al. (2013), where also the position is estimated. Reitsma (2010) considers the stand pipe and choke pressures for detection of influx and loss, but does not isolate the position. He argues that it is beneficial to have fault diagnosis without a coriolis flow meter downstream the choke, due to intolerance to gas flow, limited space, and vibrations offshore. In Gravdal and Lorentzen (2010), wired drill pipe is used to detect and isolate a kick in between pressure sensors.

This study is based on the methods developed in Willersrud and Imsland (2013), using an adaptive observer approach for fault diagnosis. The model and the adaptive observer used are briefly presented in Sec. 2. The methods for fault diagnosis are presented in Sec. 3, using statistical methods to detect changes in estimated parameters. Some details about the flow loop are presented in in Sec. 4, and the fault diagnosis framework is demonstrated in Sec. 5 showing the main results. The results are discussed in Sec. 6 and the paper is summarized in Sec. 7.

2. DRILLING MODEL AND OBSERVER

The model of the drilling system used in this study is a simplified hydraulics model (Kaasa et al., 2012) with two control volumes, one for the drillstring and one for the annulus, connected through the drill bit. See Fig. 1 for a schematic overview. The model is represented by the ordinary differential equations

$$\frac{dp_p}{dt} = \frac{\beta_d}{V_d}(q_p - q_{\text{bit}}) \tag{1a}$$

$$\frac{dp_c}{dt} = \frac{\beta_a}{V_a}\left(q_{\text{bit}} + q_{\text{bpp}} - q_c\right) \tag{1b}$$

$$\frac{dq_{\text{bit}}}{dt} = \frac{1}{M}\left(p_p - p_c - F(\theta, q_{\text{bit}}) - (\rho_a - \rho_d)gh_{\text{TVD}}\right) \tag{1c}$$

where p_p is the drilling pump pressure, p_c is the choke pressure, and q_{bit} the flow through the bit. The parameter β is the bulk modulus, V is the volume, and ρ is the density in the control volume. Subscripts d and a denote the drillstring and annulus control volumes, respectively. The constant g is the gravitational acceleration. The parameter M is the integrated density over the cross section A, giving an integrated value over the segment $\Delta L_i = L_i - L_{i-1}$ as

$$M_i = \int_{L_{i-1}}^{L_i} \frac{\rho_i(x)}{A_i(x)} dx.$$

The total integrated value from the the pump to the choke is $M = M_d + M_a$. Furthermore, the true vertical depth h_{TVD} is assumed known.

The choke flow can be represented by the choke equation

$$q_c = \theta_c C_v g(u_c)\sqrt{p_c - p_{c,0}}$$

where C_v is the choke constant, u_c is the choke opening, and $p_{c,0}$ is pressure downstream the choke. The choke characteristics $g(u_c)$ is found experimentally. The parameter θ_c represents possible choke plugging, and is nominally equal to 1. The total friction $F(\theta, q_{\text{bit}})$ is given by

$$F(\theta, q_{\text{bit}}) = (\theta_d + \theta_b + \theta_{a1} + \theta_{a2} + \theta_{a3} + \theta_{a4})q_{\text{bit}}^2 \tag{2}$$

which is the sum of friction in the drillstring, bit, and annular sections between pressure measurements, respectively. This friction model is best matched when there is turbulent flow of a Newtonian fluid. The vector of unknown parameters is

$$\theta = [\theta_d,\ \theta_b,\ \theta_{a1},\ \theta_{a2},\ \theta_{a3},\ \theta_{a4},\ \theta_c]^\top. \tag{3}$$

The relationship between the wired drill pipe pressure measurements and the annular friction is given by

$$p_{\text{bit},0} = p_p - \theta_d q_{\text{bit}}^2 + G_d(\rho_d) \tag{4a}$$

$$p_{\text{bit}} = p_{\text{bit},0} - \theta_b q_{\text{bit}}^2 \tag{4b}$$

$$p_1 = p_c + \theta_{a1} q_{\text{bit}}^2 + G_1(\rho_a) \tag{4c}$$

$$p_2 = p_1 + \theta_{a2} q_{\text{bit}}^2 + G_2(\rho_a) \tag{4d}$$

$$p_3 = p_2 + \theta_{a3} q_{\text{bit}}^2 + G_3(\rho_a) \tag{4e}$$

$$p_{\text{bit}} = p_3 + \theta_{a4} q_{\text{bit}}^2 + G_4(\rho_a) \tag{4f}$$

where $G_i(\rho_a) = \rho_a g(h_{i-1} - h_i),\ i \in 1, \ldots, 4$ is the hydrostatic pressure difference between the two measurement points in the annulus, and $G_d = \rho_d g h_{\text{TVD}}$ is the hydrostatic pressure in the drillstring. It is assumed that h_i is known.

Note that in Willersrud and Imsland (2013) the formation of a pack-off giving unknown annular friction parameters was studied, but where it was assumed that the bit and drillstring parameters were known. In this paper there are possible faults such as bit plugging and drillstring washout, making it necessary to also have unknown bit and drillstring parameters.

The adaptive observer in Willersrud and Imsland (2013), which is based on Besançon (2000), is used to estimate states and parameters. The system above can be written on the form

$$\dot{x} = \alpha(x, z, u) + \beta(x, z, u)\theta \tag{5a}$$

$$z = \eta(x, z, u) + \lambda(x, z, u)\theta \tag{5b}$$

where $x(t) \in \mathbb{R}^n$ are the states, $z(t) \in \mathbb{R}^m$ are additional measurements, $u(t) \in \mathbb{R}^p$ are the inputs, $\theta \in \mathbb{R}^q$ are unknown parameters we want to estimate, and

$\alpha(\cdot)$, $\beta(\cdot)$, $\eta(\cdot)$ and $\lambda(\cdot)$ are locally Lipschitz. Specifically, $x = [p_p,\ p_c,\ q_{\text{bit}}]^\top$, $z = [\ p_{\text{bit},0},\ p_{\text{bit}},\ p_1,\ p_2,\ p_3,\ p_{\text{bit}}]^\top$, $u = [q_p,\ q_{\text{bpp}},\ u_c]^\top$, and with system matrices

$$\alpha(x,u) = \begin{bmatrix} -\dfrac{\beta_d}{V_d}(x_3 - u_1) \\ \dfrac{\beta_a}{V_a}(x_3 + u_2) \\ \dfrac{1}{M}(x_1 - x_2 - (\rho_a - \rho_d) g h_{\text{TVD}}) \end{bmatrix} \tag{6a}$$

$$\eta(x,z) = [x_1 + G_d,\ z_1,\ x_2 + G_1, \dots \tag{6b}$$

$$z_3 + G_2,\ z_4 + G_3,\ z_5 + G_4]^\top \tag{6c}$$

$$\beta(x,u) = [\beta_3\ \beta_3\ \beta_3\ \beta_3\ \beta_3\ \beta_3\ \beta_2] \tag{6d}$$

$$\lambda(x) = [\lambda_1\ \lambda_2\ \lambda_3\ \lambda_4\ \lambda_5\ \lambda_6\ 0] \tag{6e}$$

where $\beta_2 = \frac{\beta_a}{V_a}\left[0, -C_v g(u_3)\sqrt{x_2 - p_{c,0}}, 0\right]^\top$, $\beta_3 = \frac{1}{M}\left[0, 0, -x_3^2\right]^\top$, $\lambda_1 = \lambda_2 = -x_3^2 e_j$, and $\lambda_3 = \lambda_4 = \lambda_5 = \lambda_6 = x_3^2 e_j$, where e_j is the jth column of the identity matrix $I_6 \in \mathbb{R}^{6\times 6}$.

Theorem 1. Given an observer for system (5) on the form

$$\dot{\hat{x}} = \alpha(x,z,u) + \beta(x,z,u)\hat{\theta} - K_x(\hat{x} - x) \tag{7a}$$

$$\dot{\hat{\theta}} = -\Gamma\beta^\top(x,z,u)(\hat{x} - x) - \Lambda\lambda^\top(x,z,u)(\hat{z} - z) \tag{7b}$$

$$\hat{z} = \eta(x,z,u) + \lambda(x,z,u)\hat{\theta} \tag{7c}$$

where $K_x, \Lambda, \Gamma > 0$ are tuning matrices, and assume $\dot{\theta} = 0$. Let $e_x = \hat{x} - x$ and $e_\theta = \hat{\theta} - \theta$ be variables for the error dynamics, where $e = [e_x^\top, e_\theta^\top]^\top = 0$ is an equilibrium point. Then $e = 0$ is globally exponentially stable if

$$\Gamma^{-1}\Lambda\lambda^\top(\cdot)\lambda(\cdot) - \beta^\top(\cdot)K^\top K\beta(\cdot) > kI_q \tag{8}$$

for some constant $k > 0$, where $I_q \in \mathbb{R}^{q\times q}$ is the identity matrix, and $K = \frac{1}{2}\left(I_n - K_x^{-1}\right)$.

See Willersrud and Imsland (2013) for proof of Thm. 1. Note that the assumption $\dot{\theta} = 0$ is made to facilitate in the convergence proof of the observer. In reality there are faults and measurement noise, making θ stochastic.

3. FAULT DIAGNOSIS

Fault diagnosis is a term which typically describes methods for detecting a fault, isolating its location, and identifying the type of fault. Common for fault diagnosis methods is that they rely on some residual sensitive to faults and preferably insensitive to disturbances and modeling uncertainties (Blanke et al., 2006; Ding, 2008). The residual is typically designed to give zero value at the fault-free normal case, and a nonzero value during a fault. Ding (2008) describes two strategies to evaluate the residual. One of them is norm based evaluation using robust control theory. Another one is statistic testing using statistical methods, which is used in this paper.

By estimating friction parameters throughout the system it is possible to differentiate between pressure losses due to change in flow from change in friction. If we then classify sets of parameter changes it is possible to identify the kind of fault, and to some extent its location. The friction parameters can be estimated by an adaptive observer, such as the one described in Sec. 2. In order to have residuals sensitive to parameter changes with zero value for the nominal case and nonzero for a faulty case, a change detection algorithm is employed.

3.1 Change detection algorithms

The data used in this paper is quite noisy, and thus a statistical evaluation of the estimated parameters (3) is used to detect changes. These methods assume some known probability distribution $p_\theta(y)$ of a random variable y with known parameter $\theta = \theta_0$ for the fault-free case $\mathcal{H}_0$ and some known or unknown parameter θ_1 for the fault case $\mathcal{H}_1$. If θ_1 is known, the cumulative sum (CUSUM) type of algorithms can be used, if not the generalized likelihood ratio (GLR) is typically applied. An excellent overview of these algorithms is given in Basseville and Nikiforov (1993).

A change between the two hypotheses

$$\begin{aligned} \mathcal{H}_0 &: \theta(i) = \theta_0 \quad \text{for} \quad 1 \le i \le k \\ \mathcal{H}_1 &: \theta(i) = \theta_0 \quad \text{for} \quad 1 \le i \le k_0 \text{ and} \\ &\quad\ \theta(i) = \theta_1 \quad \text{for} \quad k_0 \le i \le k \end{aligned}$$

at time k_0 is detected if a decision function $g(k)$ increases above a threshold h, namely

$$\begin{aligned} &\text{if} \quad g(k) \le h \quad \text{accept} \quad \mathcal{H}_0, \\ &\text{if} \quad g(k) > h \quad \text{accept} \quad \mathcal{H}_1. \end{aligned}$$

The log-likelihood between the known and unknown parameter is an expression for the probability of y having either parameter value θ_0 or θ_1 and is given by

$$S_j^k(\theta_1) = \sum_{i=j}^{k} \ln \frac{p_{\theta_1}(y(i))}{p_{\theta_0}(y(i))} \tag{9}$$

where k is the current sample time (Blanke et al., 2006). With both change time k_0 and parameter θ_1 unknown the GLR decision function is given by

$$g(k) = \max_{k-N+1 \le j \le k} \max_{\theta_1} S_j^k(\theta_1), \tag{10}$$

where we use a window of size N of the data series. If $p_\theta(y)$ is Gaussian and the variance known, the decision function is given by

$$g(k) = \frac{1}{2\sigma^2} \max_{k-N+1 \le j \le k} \frac{1}{k - j + 1}\left[\sum_{i=j}^{k}(y(i) - \mu_0)\right]^2 \tag{11}$$

which we will assume for the parameters in this paper. In addition, we will use $\text{sgn}(g(k)) = \text{sgn}(\mu_0 - \hat{\mu}_1)$ to determine in which direction the parameter is moving. An underlying assumption is that Gaussian parameter estimates is a reasonable approximation.

3.2 Fault isolation and identification

In the previous section it was discussed how to detect a change in a parameter. A change due to a fault is called a symptom (Isermann, 2006; Ding, 2008). Since the different faults generate different symptoms, it may be possible to isolate and identify an occuring fault. In Tab. 1 the faults are listed with the corresponding changes in parameters. The naming used for the faults is done in the same way as for the parameters, where fault i is a fault happening between sensor p_{i-1} and p_i. As an example, 'fluid loss 4' is a loss of fluids between sensors p_3 and p_4 in the

annulus. Following Isermann (2006); Blanke et al. (2006), we see that all faults can be uniquely identified based on the symptoms, but that two or more faults may not be identified correctly simultaneously. It is not possible to, e.g., detect fluid loss and drillstring washout simultaneously. This is not necessary a weakness in practice, since downhole faults such as the ones described in this paper are all quite severe, requiring some counter-measures to be taken. By using the GLR decision function (11) on each of

Table 1. Fault symptoms with increasing (+), decreasing (−) and unchanged (0) behavior.

	θ_d	θ_b	θ_{a4}	θ_{a3}	θ_{a2}	θ_{a1}	θ_c
Fluid loss 1	0	0	0	0	0	−	+
Fluid loss 2	0	0	0	0	−	−	+
Fluid loss 3	0	0	0	−	−	−	+
Fluid loss 4	0	0	−	−	−	−	+
Drillstring washout 1	−	−	−	−	−	−	0
Drillstring washout 2	−	−	−	−	−	0	0
Drillstring washout 3	−	−	−	−	0	0	0
Drillstring washout 4	−	−	−	0	0	0	0
Gas influx 1	0	0	0	0	0	+	−
Gas influx 2	0	0	0	0	+	+	−
Gas influx 3	0	0	0	+	+	+	−
Gas influx 4	0	0	+	+	+	+	−
Bit plugging	0	+	0	0	0	0	0
Choke plugging	0	0	0	0	0	0	−

the parameters in Tab. 1 with a threshold vector $h \in \mathbb{R}^q$, all faults can possibly be detected, isolated and identified. Note that this matrix only shows faults that are tested in the experimental setup, whereas it can easily be extended to diagnose faults such as pack-off and hole enlargement.

4. MEDIUM-SCALE FLOW LOOP

The experimental setup is a horizontal water-based flow loop of 1400 meters, designed to match a real drilling rig as closely as possible. It is developed by Statoil and set up at the International Research Institute of Stavanger in Norway. Parts of the loop is shown in Fig. 2. Pipes and equipment are full-size with a high rate conventional piston rig pump, 5 1/2"-7" outer diameter pipes, and two parallel MPD chokes. The setup can emulate faults such as gas influx, drillstring washout, loss of circulation, bit plugging, and choke plugging, see Fig. 1. In addition to topside measurements there are distributed pressure sensors, giving the same information as with wired drill pipe. The physical parameters for the flow loop used in the hydraulic drilling model (1) is given in Tab. 2.

Table 2. Parameters in the hydraulic model.

$\beta_{d,a}$	22 000 bar	Effective bulk modulus
$\rho_{d,a}$	1.0 kg/L	Drilling fluid density
M_a	0.374 bar s^2/L	Integrated density per cross section
M_d	0.581 bar s^2/L	Integrated density per cross section
V_a	13.2×10^3 L	Volume of fluid in annulus
V_d	8.56×10^3 L	Volume of fluid in drillstring
h_{TVD}	2.14 m	True vertical depth of bit
L_d, L_a	703 m	Length of drillstring/annulus

There are some aspects in a real drilling process the flow loop cannot capture. Since the pipes are horizontal, gas percolating up the annulus will not expand due to decreased hydrostatic pressure. Furthermore, since the loop consists of circular pipes, annular effects and drillstring rotation will not be captured.

Fig. 2. Flow loop with drillstring washout and gas injection (left), and fluid loss and drill bit (right).

During analysis of the data a noticeable deadband problem is found in the chokes. This can also be a problem on a real rig using an MPD control system. The servo motor angle is measured, not the actual choke opening. It will thus be a possible discrepancy between logged and actual opening which will affect the estimated choke parameter θ_c. The data is therefore filtered such that when the choke opening is going from opening to closing action, or vice versa, it must first travel the deadband distance before the opening position actually changes. Another issue in the test facility is bias on the pressure measurements, which also can occur on a real rig (Godhavn, 2010). This must be handled in order to get correct parameter estimates. An auto-calibration is applied on the pressure sensors when there is no flow, since then the pressure drop is only dependent on known hydrostatic pressure.

5. DIAGNOSIS OF EXPERIMENTAL DATA

The fault diagnosis framework in Sec. 3 is applied to a series of data sets containing the faults bit plugging, drillstring washout between sensors p_1 and p_2, fluid loss between sensors p_3 and p_4, and finally gas influx between sensors p_1 and p_2. These faults are named 'bit plugging', 'washout 2', 'loss 4', and 'gas 2', respectively. The time of the actual faults occurring are shown in the lower panel in Fig. 4. Note that this information is not known in the fault diagnosis.

State and parameter estimation. The observer is initialized with $\hat{x}(0) = [10, 20, 10]^\top$ and $\hat{\theta}_i(0) = 0$, and applied on the series of data sets which has a sample rate of 10 Hz. The observer gains used are $K_x = \text{diag}\{5, 5, 5\}$, $\Gamma = 5 \times 10^{-4} \times \text{diag}\{1, 1, 1, 1, 1, 10^2\}$ and $\Lambda = 5 \times 10^{-4} \times \text{diag}\{1, 1, 1, 1, 1, 10^2\}$, where 'diag' denotes a diagonal matrix. Tuning of observer gains are done primarily to get correct scaling. Results for the state estimation is shown in Fig. 3. Since topside pressures are measured, pressure estimation shown in the upper panel is very good as expected. Note that we measure the pump flow q_p and not the bit flow, shown in the lower panel, and that the bit flow estimate closely follows the measured pump flow. If the flow through restrictions such as the bit or the choke is different from what the model expects, there will be a change in estimates of θ_b or θ_c. This is used in the fault diagnosis framework, where, e.g., θ_c increases when there is a fluid loss. Parameter estimation is shown in

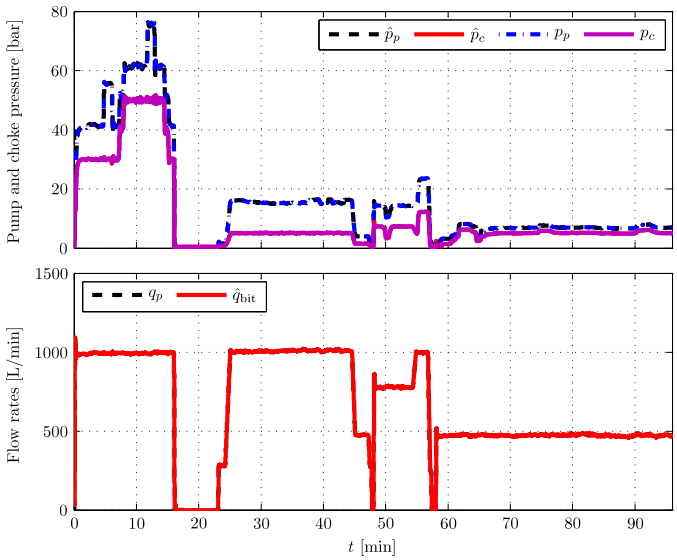

Fig. 3. State estimation of pressures and flow.

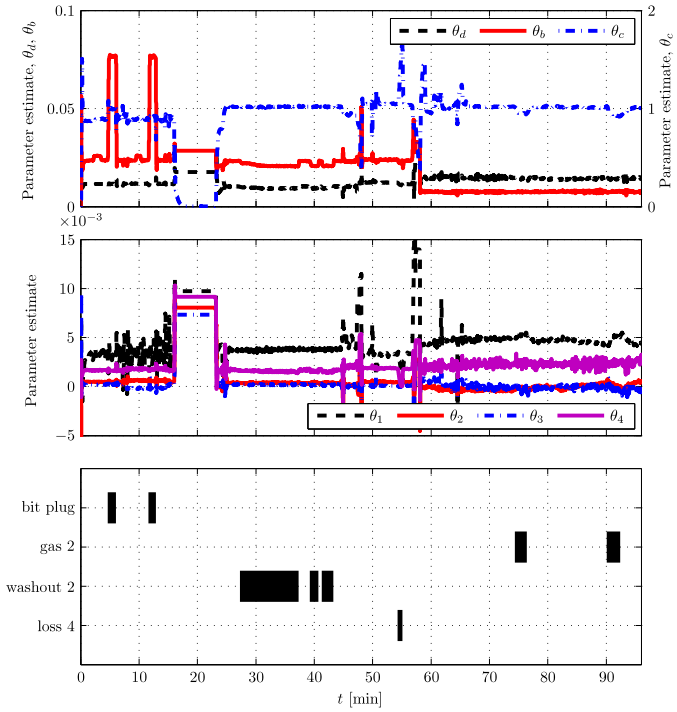

Fig. 4. Parameter estimation and true faults.

the two upper panels of Fig. 4. From these plots we see that some faults such as bit plugging is easy to identify directly, causing a large increase in θ_b at 4:38 and 11:37 minutes. Other faults can be difficult to identify, especially with noisy parameter estimates. In the same period as the bit plugging the estimate of θ_{a1} oscillates quite much, but from Tab. 1 we would not expect any changes in θ_{a1} during a plugging of the bit. This motivates the use of more sophisticated change detection algorithms.

Detection of change in parameters. The GLR decision function (11) is applied on $\hat{\theta}$ with $\hat{\mu}_0 = \mathrm{E}(\hat{\theta})$, $\hat{\sigma}_0^2 = \mathrm{VAR}(\hat{\theta})$ calculated on intervals where we assume the fault free case $\mathcal{H}_0$. Since the data sets are merged together and not recorded consecutively, there can be some differences between the sets, for example that manual chokes are slightly moved or there are some drifting bias in the measurements. We will thus use different $\hat{\mu}_0$ and $\hat{\sigma}_0$ for the different data sets in the concatenated time series. On a real rig conditions are constant or slowly varying, making it possible to get good estimates of the statistical parameters at $\mathcal{H}_0$.

The fault diagnosis threshold vector used is

$$h = [200,\ 200,\ 30,\ 30,\ 30,\ 30,\ 200]^\top$$

with an GLR window of $N = 10$ samples. We require that the threshold should be active for a successive 100 samples in order to rule out symptoms due to transients. In order to remove false alarms when changing between data sets, the fault diagnosis is disabled around the transitions. Also note that the diagnosis must be disabled when there is (close to) zero flow due to lack of persistently exciting signals ((8) not being fulfilled). Physically this can be explained by the fact that there is no friction loss when there is no flow. This can be seen in the parameter estimates in Fig. 4, which change quite drastically between 16 and 23 minutes.

Fault isolation and identification. The resulting fault diagnosis is shown in Fig. 5. This figure is generated by using the threshold h on the GLR estimates, and isolating and identifying the faults according to Tab. 1. Each row represents one kind of fault, and the true faults are indicated in black. The first faults occurring are two pluggings of the drill bit. They are correctly identified at 4:43 and 11:42 minutes, respectively, with some short instances of unidentifiable faults. The next fault is a drillstring washout starting at 27:17. The washout is gradually increasing, and identified at 30:04. Here we see that the real fault of 'washout 2' is a bit difficult to isolate, although the framework successfully identify the fault as a washout and not, e.g., a loss. The reason for the inaccuracy may be caused by the fact that detection of small changes in parameters may be lost due to noise. Also note that the position of the drillstring washout is very close to sensor p_2, meaning that the real fault could just as much be categorized as 'washout 3'. In that sense can an isolation of alternation between 'washout 3' and 'washout 4' be considered quite good. Next a very short burst of fluid 'loss 4' occurs at 54:18. The type of fault is correctly identified, although its position is not so easy to determine. Also here, the reason may be that there are small changes in the parameters. The last faults are two influxes of gas at the same well position as the washout, namely between sensor p_1 and p_2, but very close to p_2. The real fault is thus 'gas 2'. By studying Fig. 5 we see that both influxes are detected as some faults. The first one is clearly identified as 'gas 1', meaning that we see some change in θ_{a1} but not θ_{a2}. Again, this can be caused by a small signal to noise ratio. The next influx is more unclear. Here it is an indication that the cause of parameter change is due to gas in the system. For some samples, it is identified as 'gas 1', for others its position is uncertain, and for the rest the type of fault is also uncertain.

6. DISCUSSION

In the fault diagnosis in Sec. 5 it can be seen that the different faults are correctly identified and to some extent its position is estimated as well. Moreover, there may be some delay between the time of fault occurrence

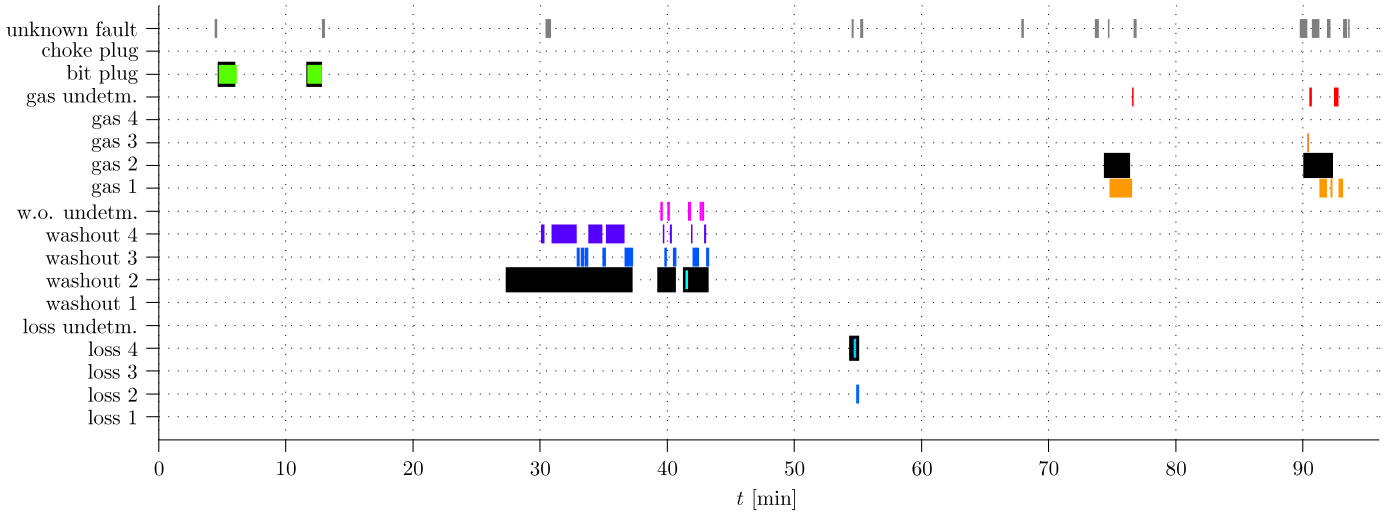

Fig. 5. Fault identification: Bit plugging, drillstring washout, fluid loss and gas kick. True faults are indicated in black.

and detection. One of the reasons is that the method in this paper is somewhat sensitive to parameter estimation, where a good estimate of the fault free case $\mathcal{H}_0$ is required. If the parameter estimation has much noise, changes will not be detected. Hence will there be a tuning trade-off between false and missed fault detection.

The fault diagnosis framework in this paper is tested in a flow loop with full-size equipment such as rig pump and chokes, as well as long pipes with typical diameters. It is thus believed that the method could be applied on a real rig with managed pressure drilling installed. A significant difference is that a real rig will have a true vertical depth of up to several thousand meters. This will change the conditions during a gas influx drastically. If the drilling fluid is oil based and not water based, gas can be dissolved in the fluid at high pressure and liberated as it comes to lower depth. In addition will cuttings and non-Newtonian drilling fluid change the friction behavior. These aspects will have to be taken into consideration in a fault diagnosis system for a real rig.

7. CONCLUSION AND FUTURE WORK

A novel framework is proposed for fault detection, isolation and identification of downhole faults in managed pressure drilling. The framework is based on a simple and easy configurable hydraulic process model, a nonlinear adaptive observer, and threshold tests of generalized likelihood ratio functions. One of the challenges is to detect small changes when there are noisy signals. The method requires that we know when we are in a fault-free scenario, but it is not limited to knowing the magnitude of the faults. We apply the framework to data from a medium-scale flow loop and show that we can successfully detect and to some extent isolate and identify faults such as bit and choke plugging, drillstring washout, fluid loss, and gas kick by using distributed pressure sensors.

As future work it would be interesting to include fault estimation in the framework, i.e., estimating the magnitude of the faults, such as gas influx or fluid loss flow rate. Another improvement is to estimate the position of different faults with a larger accuracy than in between measurements.

ACKNOWLEDGMENT

Financial support from Statoil ASA and the Norwegian Research Council (NFR project 210432/E30 Intelligent Drilling) is gratefully acknowledged. Experimental data are results from ongoing internal research in the department Intelligent Drilling in Statoil RDI.

REFERENCES

Basseville, M. and Nikiforov, I.V. (1993). *Detection of Abrupt Changes: Theory and Applications*. Prentice Hall, Englewood Cliffs, NJ.

Besançon, G. (2000). Remarks on nonlinear adaptive observer design. *Systems & Control Letters*, 41(4), 271–280.

Blanke, M., Kinnaert, M., Lunze, J., and Staroswiecki, M. (2006). *Diagnosis and fault-tolerant control*. Springer, Berlin, 2nd edition.

Ding, S.X. (2008). *Model-based Fault Diagnosis Techniques*. Springer, Berlin.

Godhavn, J.M. (2010). Control Requirements for Automatic Managed Pressure Drilling System. *SPE Drilling & Completion*, 25(3), 336–345.

Gravdal, J.E. and Lorentzen, R. (2010). Wired Drill Pipe Telemetry Enables Real-Time Evaluation of Kick During Managed Pressure Drilling. SPE 132989, Brisbane, Australia.

Hauge, E., Aamo, O., Godhavn, J.M., and Nygaard, G. (2013). A novel model-based scheme for kick and loss mitigation during drilling. *Journal of Process Control*, 23(4), 463–472.

Isermann, R. (2006). *Fault-Diagnosis Systems*. Springer, Berlin.

Kaasa, G.O., Stamnes, O.N., Aamo, O.M., and Imsland, L. (2012). Simplified Hydraulics Model Used for Intelligent Estimation of Downhole Pressure for a Managed-Pressure-Drilling Control System. *SPE Drilling & Completion*, 27(1), 127–138.

Nygaard, V., Jahangir, M., Gravem, T., Nathan, E., Evans, J., Reeves, M., Wolter, H., and Hovda, S. (2008). A Step Change in Total System Approach Through Wired Drillpipe Technology. SPE/IADC 112742, Orlando, Florida.

Reitsma, D. (2010). A simplified and highly effective method to identify influx and losses during Managed Pressure Drilling without the use of a Coriolis flow meter. SPE/IADC 130312, Kuala Lumpur, Malaysia.

Willersrud, A. and Imsland, L. (2013). Fault Diagnosis in Managed Pressure Drilling Using Nonlinear Adaptive Observers. In *Proc. European Control Conference (ECC)*. Zürich, Switzerland.